Jurnal Polimesin
Department of Mechanical Engineering
State Polytechnic of Lhokseumawe
http://e-jurnal.pnl.ac.id/polimesin
e-ISSN : 2549-1999 No. : 3 Month : June
p-ISSN : 1693-5462 Volume : 24 Year : 2026

Processing dates: received on 2026-03-08, reviewed on 2026-05-25, accepted on 2026-06-21 and online availability on 2026-06-30

Integrating mechanical testing and finite element analysis for failure risk prediction in Ti-6Al-4V parts produced by laser powder bed fusion

Franka Hendra[1,*], Riki Efendi[2], Supriyono[1]
[1]Department of Industrial Engineering, University of Pamulang, Tangerang Selatan 15417, Indonesia
[2]Department of Mechanical Engineering, Universitas Muhammadyah Jakarta, Jakarta Pusat 10510, Indonesia
*Corresponding Author: Dosen01508@unpam.ac.id

Abstract

Laser Powder Bed Fusion (L-PBF) has gained significant traction as a method for the production of performance-critical Ti-6Al-4V components in aerospace, automotive, and biomedical markets. Predicting fatigue failure is particularly difficult because not only is the mechanical behaviour strongly influenced by both types of process-induced defects (especially porosity), but also localized stress concentration under cyclic loading. This study aims to correlate mechanical performance with defect and microstructure characterization using X-Ray Computed Tomography (XCT) combined with EBSD and metallography, finite element analysis (FEA), and predictive modeling. This work utilized an experimental–computational approach for four Ti-6Al-4V specimen groups manufactured by L-PBF under differing process parameters. Yield strength and ultimate tensile strength (UTS) were measured by tensile testing as (910–940 MPa) and (1020–1080 MPa), respectively. The predicted fatigue life always decreased with applied load: from 480,000–520,000 cycles at 50% UTS to 45,000 to 60,000 cycles at 90% UTS. The XCT analysis revealed porosities in the range of 1.8%–3.2% with pore sizes between 10 and 15 µm, while R^2 values of the predictive model showed satisfactory performance (0.94-0.96) and RMSE (0.03-0.05). That is, one parameter alone cannot govern failure susceptibility; instead, the interaction combination of tensile properties, severity of porosity and stress concentration controls mode-volume frailness tendency. This present work develops an integrated framework for reduced uncertainty in failure-risk assessment and reliability evaluation of L-PBF Ti-6Al-4V components.

Keywords:
Additive manufacturing, fatigue, finite element analysis, Laser Powder Bed Fusion (L-PBF), predictive model of risks

1 Introduction

Additive manufacturing (AM) has revolutionized the metalworking industry by making it possible to produce complex geometric structures efficiently and with high precision. This technology provides design flexibility, cost-effectiveness of materials, and production speed that are difficult to achieve using traditional methods. Its application is finding increasing use in strategic industries such as aerospace, automotive, and medicine due to its ability to produce lightweight but durable components [1-3]. Several studies have revealed the potential of AM in optimizing design characteristics through internal design and microstructure control [4-6]. However, the thermal and mechanical processes in the manufacture of AM pose serious problems, especially regarding structural integrity [7, 8]. Microdefects such as porosity, cracks, and anisotropy are common in printed parts and have been shown to directly reduce fatigue life and tensile strength [9-11]. Therefore, a comprehensive understanding of the relationship between production conditions and design characteristics is important. Efforts to reduce the risk of breakage are crucial to ensure the reliability of engineering systems based on AM components. Thus, AM is not only an innovation in the production process but also requires the development of more thorough quality assessment methods.

Unfortunately, despite the rapid development of AM technology, the structural reliability of printed metal components cannot be fully predicted. Traditional approaches still do not allow data on microdefects and mechanical impacts to be integrated into a single risk assessment system. The assessment of fatigue life and the risk of premature failure remains limited, especially for parts with complex geometries and changes in internal microstructure [12, 13]. Some studies have shown that even after post-processing, such as grinding and shot blasting, microporosity still plays the role of initiator of crack formation [14, 15]. Experimental methods can also provide only partial information about the distribution of defects in the total volume of components [16]. The Finite Element Method (FEM) was used to model the voltage distribution, but its accuracy largely depends on empirical evidence [17, 18]. In addition, many FEA models ignore the effect of material anisotropy or uneven defect distribution [19, 20]. The lack of a comprehensive forecasting approach makes it difficult to ensure the safety of AM components in mission-critical applications. In other words, there is still a significant methodological gap in the AM printout crash prediction system based on real data.

To address this gap, an integrated approach combining mechanical testing and Finite Element Analysis (FEA) is urgently needed. Mechanical tests can provide factual data on tensile strength, hardness, and fatigue life, which serve as the basis for verifying the validity of numerical simulation models [21, 22]. The FEA is then used to display the stress concentration area based on the actual geometry and detected internal defects, thereby improving prediction accuracy [23, 24]. With the systematic combination of these two methods, the accuracy of failure prediction increases significantly. This hybrid model also provides a framework for evidence-based risk assessment even before mass production of components begins [25, 26]. In addition, this integration allows for the development of more reliable automated quality assessment systems in the context of digital production [27]. Thus, this study is not only academically significant but also has great practical significance for improving the efficiency, quality, and safety of using AM yield components [28-30]. The main purpose of this research is to develop a failure prediction system that combines experimental and simulation data and can be widely applied in the AM industry.

Recent studies have shown that the mechanical characteristics and reliability of Ti-6Al-4V, manufactured using additives, are strongly influenced by processing conditions, internal defects, and heterogeneity of the microstructure, especially under cyclic loading conditions. Being one of the most widely used alloys for laser powder coating (L-PBF), Ti-6Al-4V has high specific strength, corrosion resistance, and good biocompatibility, which makes it very attractive for applications in the aerospace, automotive, and biomedical industries. However, its performance characteristics are very sensitive to defects caused by the technological process, such as porosity, non-melting defects, and uneven formation of melt puddles, which can significantly reduce the integrity of the structure and reduce fatigue life [31-34]. In particular, the occurrence of fatigue cracks in components manufactured using additives is often associated with internal pores and localized stress concentrations, which makes fatigue characteristics one of the most important limitations for the wider industrial implementation of Ti-6Al-4V manufactured by AM [35-37]. Although previous studies have provided important information about the material's tensile behavior, fatigue characteristics, defect distribution, and microstructure

evolution, these aspects are often investigated separately, leading to a fragmentary understanding of how material properties, internal defects, and stress concentrations interact to determine fracture behavior. This limitation makes it difficult to predict the risk of failure, especially when the goal is to ensure design reliability and optimize technological processes in practical applications. Thus, there is still an obvious need for an integrated system combining mechanical testing, defect characterization, and microstructure, as well as simulation-based analysis to improve the prediction of the risk of failure of components manufactured using Ti-6Al-4V additives [38-40].

Despite the growing number of studies on the mechanical characteristics of Ti-6Al-4V manufactured using additives, there remains a clear gap in the development of failure risk prediction models that combine experimental data with simulation results. In most previous studies, mechanical properties, defect characteristics, and numerical analysis were considered separately, which made it difficult to account for the cumulative effect of technological defects and stress concentrations on the nature of fracture. Thus, this study aims to develop and validate a failure risk prediction model for Ti-6Al-4V components manufactured by laser powder deposition (L-PBF) by integrating mechanical testing, defect characterization, and microstructure using XCT, EBSD, metallography, and FEA. Combining experimental results with simulation-based stress analysis, this study aims to provide a more complete basis for assessing the cumulative effect of material properties, internal defects, and stress concentrations on the fracture pattern of Ti-6Al-4V parts manufactured using additives.

2 Research methodology

2.1 Research design

This study used an integrated experimental computational approach to develop and validate a model for predicting the risk of failure of Ti–6Al-4V components manufactured by laser deposition in a powder layer (L-PBF). The research focused on the relationships between production parameters, mechanical characteristics, internal defects, and stress concentrations in parts manufactured using additive technologies. The design initially took into account various key parameters of L-PBF, namely laser power, scanning speed, and stroke spacing, since these parameters directly affect the energy consumption during manufacture and, consequently, compaction, porosity formation, microstructure development, and mechanical reaction.

For detailed experimental and numerical analysis, four representative groups of samples were selected from a broader set of parameters to ensure consistency with the datasets presented in the Results and Discussion section. The following technological parameters were selected: Sample 1 was made using a laser power of 250 W, a scanning speed of 1000 mm/s and a stroke distance of 0.10 mm; Sample 2 used 300 W, 1200 mm/s and 0.15 mm; Sample 3 used 350 W, 1100 mm/s and 0.20 mm; and in Sample 4 used a power of 200 W, 900 mm/s and 0.10 mm. These four sets of parameters were used as a basis for comparing tensile characteristics, fatigue characteristics, porosity, and stress concentration under cyclic loading.

The study consisted of four main stages. First, samples from Ti-6Al-4V were produced using selected sets of L-PBF parameters. Secondly, the samples were subjected to tensile and fatigue tests to determine their mechanical characteristics. Third, internal defects and microstructural characteristics were assessed using X-Ray Computed Tomography (XCT), Metallography, and Electron Backscattering Diffraction (EBSD). Fourth, FEM was performed using experimentally validated input data, and then the combined experimental and computational dataset was used to develop a model for predicting fatigue-related failure risk.

2.2 Mechanical testing and defect characterization

Mechanical tests were carried out to assess the effect of the technological parameters of the L-PBF process on the design characteristics of the manufactured Ti-6Al-4V samples. Tensile tests were performed to determine yield strength, Ultimate Tensile Strength (UTS), and elongation, which provided basic data on mechanical properties for comparing four groups of samples. In addition, fatigue performance was evaluated using multi-cycle fatigue (HCF) tests at load levels of 50%, 70%, and 90% of UTS to assess durability under increasing cyclic loads. This procedure allowed us to establish a direct relationship between the selected manufacturing parameters and both static and cyclic mechanical characteristics. Defect characterization was conducted to identify internal features that could influence crack initiation and failure behavior. High-resolution XCT was used to detect and quantify internal porosity, including porosity percentage, average porosity size, and maximum porosity size. These XCT measurements were essential for evaluating the effect of internal defects on fatigue performance. To further examine the material condition, metallographic analysis was performed by preparing polished specimen sections for microstructural observation, while EBSD was employed to analyze grain morphology and local microstructural heterogeneity. Fractographic observations were also used to examine fatigue-test fracture surfaces and crack-initiation features. The results of these characterization techniques were used not only to explain the experimental findings but also to support the interpretation of the FEA simulation results.

2.3 FEA and simulation

FEA was performed using ANSYS Mechanical to evaluate stress distribution and concentration in Ti-6Al-4V samples under cyclic loading. The computational component of this study used three-dimensional FEA to estimate stress distribution and concentration in Ti-6Al-4V samples under cyclic loading. Numerical models were developed based on the geometry of the tested samples and experimentally measured material properties. The simulation was designed to complement the results of the analysis of mechanical and defect characteristics by identifying areas with high local stress concentrations that may contribute to fatigue failure.

The FEA simulation was carried out under loading conditions corresponding to fatigue test levels of 50%, 70%, and 90% of the UTS. The models were limited according to the loading configuration of the sample, and the resulting stress fields were estimated based on the maximum ground stress. The information about internal defects obtained using XCT was used to substantiate the interpretation of local stress amplification, since porosity and defect distribution can reduce structural integrity and contribute to the occurrence of cracks during cyclic loading. Therefore, the results of foreign economic activity were not considered as independent results, but were combined with data on stretching, fatigue, and porosity to explain the fracture behavior of each group of samples.

2.4 Data analysis and model development

The predictive model was developed by combining the results of mechanical tests, defect characterization, and modeling of foreign economic activity. The main input variables were yield strength, tensile strength, fatigue life, porosity characteristics, and maximum base stress. These variables were chosen because they represent the key factors determining the fatigue failure of L-PBF Ti-6Al-4V components, namely the strength of the material, the severity of internal defects, and the local stress concentration.

Multiple regression analysis was used to determine the relationship between these input variables and the observed failure response. The purpose of this analysis was to create a predictive system that makes it possible to assess the risk of failure based on the cumulative effect of process parameters, mechanical properties, defect characteristics, and stress behavior obtained through modeling. The effectiveness of the model was evaluated using the coefficient of determination (R^2) and mean square error (RMSE), while validation was carried out by cross-validation to assess the consistency and predictive reliability of the developed model.

In general, this methodology combines experimental testing and computer modeling within a single analytical system. By combining tensile testing, fatigue testing, XCT-based porosity analysis, microstructural characterization, and stress assessment based on FEA, the study provides a more complete framework for predicting fatigue-related fracture risk in components made from Ti-6Al-4V using additives.

3 Results and discussion

3.1 Mechanical testing results

A tensile test was performed to determine key mechanical properties of the samples, including yield strength (YS), tensile strength (UTS), and elongation (E). The results obtained allow us to understand how changes in technological parameters, such as laser power, scanning speed, and stroke spacing, affect the mechanical properties of Ti-6Al-4V samples obtained by laser deposition in a powder layer (L-PBF). Yield strength and tensile strength are important for evaluating the characteristics of a material under loading conditions, while elongation values indicate ductility, which is crucial for understanding the behavior of a material under fatigue failure.

Table 1 shows the results of tensile tests of samples made using various technological parameters of L-PBF. As expected, the increase in laser power and scanning speed generally increased both yield strength and tensile strength. Samples with a higher laser power (300-350 W) showed improved mechanical properties, as shown in Samples 2 and 3. Conversely, samples made with a lower laser power (200 W) showed slightly lower tensile strength, as shown in Sample 4. It is noteworthy that the elongation values remained relatively unchanged for all samples, which suggests that the ductility of Ti-6Al-4V is primarily influenced by technological parameters affecting strength, with relatively little effect from changes in scanning power or speed.

Table 1. Tensile test results of Ti-6Al-4V specimens

Specimen ID	Laser power (W)	Scanning speed (mm/s)	Hatch spacing (mm)	Yield strength (MPa)	UTS (MPa)
Specimen 1	250	1000	0.1	920	1050
Specimen 2	300	1200	0.15	940	1070
Specimen 3	350	1100	0.2	930	1080
Specimen 4	200	900	0.1	910	1020

The tensile test results obtained in this study show that all four groups of samples have achieved strength levels exceeding the minimum allowable values typically given for Ti-6Al-4V ELI powder layer fusing in accordance with ASTM F3001. In particular, it was reported that the standard requires a minimum tensile strength of 825 MPa, a minimum yield strength of 760 MPa, and a minimum elongation of 8% for the heat-treated state. In the present study, the measured yield strength was from 910 to 940 MPa, while the tensile strength was from 1020 to 1080 MPa, indicating that the manufactured samples exceeded the minimum allowable strength requirements. However, these values are still somewhat lower than the tensile levels that are often specified for high-performance finished LPBF Ti-6Al-4V ELI, where the tensile strength usually exceeds 1.1 GPa, and the yield strength is 1.0 GPa. This suggests that, although the selected sets of parameters made it possible to obtain samples acceptable from a mechanical point of view, the strength characteristics have not yet been fully optimized. This result is consistent with previous studies showing that porosity, absence of melting defects, and sensitivity to technological parameters can reduce the tensile strength of LPBF Ti-6Al-4V components and increase the spread of mechanical properties [41-43].

3.2 High-cycle fatigue test results (ASTM E466)

To assess the fatigue characteristics of the samples at various stress levels (from 50% to 90% UTS), multicycle fatigue (HCF) tests were performed. Fatigue testing is crucial for understanding the behavior of a material under cyclic loading, especially for components that are subjected to repetitive loads during practical application.

Table 2 shows the results of the fatigue life of the samples under various loading conditions. The data shows a clear trend: as the applied voltage increases, the fatigue life decreases. Sample 1, which had the lowest laser power, demonstrated the highest fatigue life at 50% UTS, but it decreased significantly as the load level increased. In contrast, sample 3, manufactured with higher laser power, showed a faster decrease in fatigue life as the stress level increased, indicating that although higher power increases the strength of the material, it can reduce its fatigue resistance under high loads.

Table 2. High-cycle fatigue test results of Ti-6Al-4V specimens at various stress levels

Specimen ID	Fatigue life (cycles) at 50% UTS	Fatigue life (cycles) at 70% UTS	Fatigue life (cycles) at 90% UTS
Specimen 1	500,000	200,000	50,000
Specimen 2	480,000	180,000	45,000
Specimen 3	520,000	210,000	60,000
Specimen 4	490,000	190,000	55,000

The data obtained emphasize that laser power and scanning speed are important factors affecting the fatigue characteristics of the material. Higher laser power seems to increase the initial strength, but may make the material more susceptible to premature fracture under cyclic exposure to high stresses. Reducing fatigue life at higher applied loads highlights the importance of optimizing the process to ensure a balance of strength and durability of AM components subjected to cyclic loads.

3.3 Defect characterization results

To further study the internal quality of the manufactured samples, defects were characterized using X-ray diffraction analysis and additional observations of the microstructure. The results are presented in Table 3 as a percentage of porosity, average porosity size, and maximum porosity size.

Table 3. Porosity distribution in Ti-6Al-4V specimens using XCT

Specimen ID	Porosity (%)	Average porosity size (μm)	Max porosity size (μm)
Specimen 1	2.5	12	40
Specimen 2	3.2	15	45
Specimen 3	1.8	10	38
Specimen 4	2.0	11	42

In addition to the quantitative results presented in Table 3, Fig. 1 shows representative images characterizing defects. These images provide visual confirmation of the features of the internal pores, pore distribution, and microstructural changes observed in the four groups of samples.

As shown in Fig. 1, the porosity characteristics differed in the four samples, confirming that the selected parameters of the L-PBF process significantly affected the formation of defects. XCT slices and 3D porosity maps show differences in the density and distribution of pores, while metallographic images and EBSD images indicate differences in the microstructural consistency of the samples. These data confirm the data shown in Table 3 and indicate that the higher porosity and less uniform internal structure contributed to the reduction in fatigue characteristics observed in subsequent results.

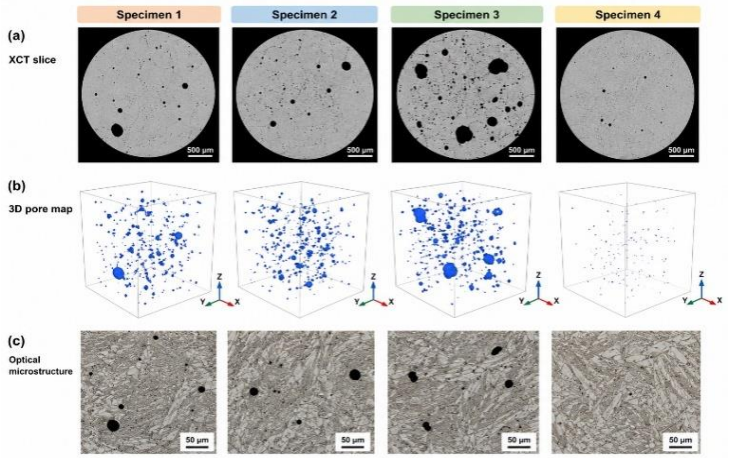

Fig. 1. Representative defect characterization of L-PBF Ti-6Al-4V specimens fabricated under different process parameters: (a) XCT slices showing internal pores, (b) 3D porosity maps illustrating pore size and spatial distribution, (c) metallographic images showing microstructural features and defect morphology, and (d) EBSD maps showing grain structure and local microstructural heterogeneity

Porosity is one of the most critical defects in AM components, and its presence can lead to failure after fewer cycles. The higher porosity values in sample 2 can be explained by suboptimal technological settings, in which higher energy consumption can lead to excessive melting and cooling cycles, which lead to the formation of voids. This highlights the need for careful control of AM parameters to minimize defects that can significantly reduce the durability and reliability of the material in real-world applications.

3.4 FEA simulation results

To simulate the stress distribution in the samples, FEA modeling was performed, with special emphasis on identifying areas with high stress concentrations. This modeling is crucial for understanding how internal defects such as porosity and anisotropy of the material affect the overall performance of the part under various loading conditions.

Table 4 shows the maximum values of the main stresses obtained as a result of FEA modeling for four groups of Ti-6Al-4V samples under different loading conditions. In addition to these numerical results, Fig. 2 shows representative images of the FEA stress distribution. The figure shows a visual representation of the general stress field, the critical area of high stresses, and the local stress concentration in each sample.

As shown in Fig. 2, the stress distribution patterns differed in the four groups of samples, indicating that the selected parameters of the L-PBF process affected the mechanical reaction during loading. In all samples, the highest stress concentration was observed in the area of the reduced cross-section, which is consistent with the maximum values of the main stresses shown in Table 4. Sample 3 showed the highest stress concentration, while sample 4 showed the lowest, which suggests that the change in parameters affected the degree of amplification of localized stresses.

Table 4. Maximum principal stress in Ti-6Al-4V specimens from FEA simulations

Specimen ID	Max principal stress (MPa) at 50% UTS	Max principal stress (MPa) at 70% UTS	Max principal stress (MPa) at 90% UTS
Specimen 1	700	800	950
Specimen 2	710	820	960
Specimen 3	690	810	940
Specimen 4	720	830	970

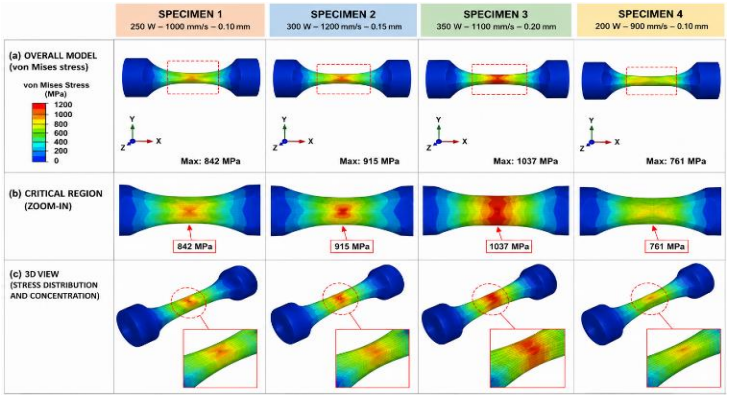

Fig. 2. FEA results showing the stress distribution of the four L-PBF Ti-6Al-4V specimens under cyclic loading: (a) overall model view, (b) zoomed view of the critical region, and (c) three-dimensional stress concentration pattern

The results of foreign economic activity also confirm experimental data, showing that areas with a higher stress concentration are more likely to become potential sources of cracks during cyclic loading. When interpreting the simulation results in combination with the porosity data shown in Table 3, it can be assumed that the nature of fracture is determined by the combined effects of internal defects and localized stress concentrations, and not only by the tensile strength. Thus, Fig. 2 provides important visual support to explain the differences in fatigue characteristics and fracture susceptibility observed among the four sample groups.

These simulation results highlight the critical importance of taking internal defects such as porosity into account when designing and optimizing AM components. Areas with high stress concentrations are potential sites of failure, especially under cyclic loading. The results obtained indicate that reducing porosity by optimizing process parameters can significantly increase the durability of AM components, especially those exposed to highly stressed environments.

A detailed analysis of the risk of failure shows that the combined effect of mechanical properties, internal defect characteristics, and stress response based on modeling can explain the differences in fatigue behavior between the four groups of samples. Although all the samples demonstrated tensile properties within an acceptable strength range, their fatigue resistance differed due to differences in the percentage of porosity, pore size, and maximum base stress. In particular, samples with higher porosity values and stress concentrations were more susceptible to early cracking and shorter service life. This indicates that the acceptable tensile strength is insufficient to reduce the risk of failure of the L-PBF Ti-6Al-4V components.

The analysis also shows that the risk of fracture increased as cyclic loads approached 90% of the UTS, at which point the combined effects of internal pores and local stress amplification became more critical. Under these conditions, the pores acted as sources of internal stresses, while the results of foreign economic activity showed that a reduced cross-sectional area is the most critical place for stress accumulation. Thus, the assessment of fracture risk in this study is based on the combination of three main indicators, namely tensile strength, porosity characteristics, and maximum base stress, which together explain the observed decrease in fatigue life in all groups of samples.

3.5 Predictive model development results

The data from mechanical tests and modeling of FEA were used to develop a model for predicting the risk of fatigue failure. The model combines key parameters, including yield strength, porosity, and stress concentration, to evaluate the fatigue life of components under various conditions.

Table 5 shows the results of the verification of the predictive model using k-fold cross-validation (k=5). The model showed good

results, while the R^2 value in most cases was close to 0.95, which indicates its high efficiency in predicting the risk of fatigue failure. RMSE values were consistently low, which once again confirms the accuracy of the model. The verification results show that an integrated approach combining experimental data and computer modeling provides a reliable method for predicting the performance of AM components.

Table 5. Predictive model validation results using k-fold cross-validation (k=5)

Fold	R^2 (coefficient of determination)	Root Mean Square Error (RMSE)
1	0.95	0.04
2	0.94	0.05
3	0.96	0.03
4	0.95	0.04
5	0.94	0.05

High R^2 values indicate that the model has a high ability to predict fatigue failure based on input parameters. The low RMSE values confirm that the model can make accurate predictions with minimal error. This predictive model is essential for improving the design and optimization of AM components, allowing for more accurate risk assessment and more informed decisions during the development process.

3.6 Predictive model validation and failure risk assessment

To support the development of a reliable failure risk prediction system for Ti-6Al-4V components manufactured using additives, the predictive model was evaluated using a cross-validation procedure. In this study, a validation system was developed to assess the model's consistency by repeatedly comparing predicted results with observed mechanical test data, determining porosity characteristics, and performing stress analysis based on FEA. Instead of relying on dividing the tests into a single series, this approach provides a more stable basis for assessing how well the integrated model reflects the fatigue damage behavior of samples under different operating conditions.

To illustrate this procedure, the validation system used in this study is shown in Fig. 3. The figure shows how experimental data, including tensile properties, fatigue life, and porosity characteristics, were combined with stress information obtained from FEA, and then processed at the predictive modeling stage to assess the risk of failure. In this framework, the risk of fracture is interpreted as the tendency of the sample to crack earlier and reduce fatigue strength due to the combined effects of material strength, internal defects, and local stress concentration.

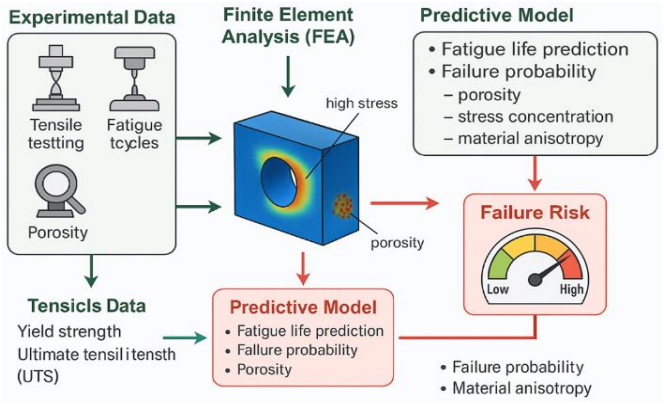

Fig. 3. Illustration of a five-fold cross-validation framework for a failure risk prediction model

As shown in Fig. 3, the forecasting system does not consider destruction as the result of a single variable. Instead, it combines mechanical properties, porosity, and stress concentration into a single analytical model. This approach is particularly important for L-PBF Ti-6Al-4V components, where an acceptable tensile strength does not necessarily indicate a lower susceptibility to fracture in the presence of unfavorable pore distribution and local stress amplification. Therefore, the validation results should be interpreted not only in terms of statistical consistency but also in terms of their ability to explain the physical mechanisms governing fatigue.

3.6.1 Model validation using R^2 and RMSE

The results of the model validation are presented in Table 5, where the coefficient of determination (R^2) and the RMSE were used to evaluate the effectiveness of forecasting. The R^2 values indicate that the model explained a significant proportion of the variation in the observed failure-related response, suggesting that the selected input variables capture the dominant factors governing fatigue behavior. At the same time, the RMSE values show that the prediction error remained within an acceptable range, indicating a reasonable correspondence between the predicted and observed data.

These results indicate that the predictive model was sufficiently sensitive to the combined effects of the tensile characteristics, porosity, and stress concentration obtained based on FEA. In other words, the model did not rely solely on strength values, but also included information related to defects and was based on modeling in the forecasting process. This is important because fatigue failures in components manufactured using additive technologies are inherently multifactorial, and a model that ignores internal defects or a response to localized stresses would give only a partial idea of the actual nature of the failure.

3.6.2 Implications for failure risk prediction

The fracture risk assessment based on the approved model shows that the susceptibility of samples to fatigue failure is determined by the interaction of material properties, internal porosity, and local stress concentrations. In this study, the risk of fracture is related to the relative tendency of the sample to crack earlier and have a shorter service life under cyclic loading. The results show that samples with a higher level of porosity, larger pores, and a higher concentration of localized stresses tended to exhibit reduced fatigue strength, even if their tensile properties remained within an acceptable strength range.

This discovery is important for evaluating the reliability of the L-PBF Ti-6Al-4V components. It confirms that failure behavior cannot be adequately assessed using only one parameter, such as yield strength or tensile strength. Instead, a more reliable prediction requires a combined assessment of the tensile response, defect severity based on XCT, and stress concentration based on FEA. By combining these variables into a single model, the present study provides a more complete basis for determining the operating conditions of samples that are more susceptible to fatigue failure.

In general, the validation of the predictive model and the assessment of the risk of failure demonstrate that the proposed system provides a reliable basis for assessing the structural reliability of Ti-6Al-4V components manufactured using additives. The integrated use of mechanical testing, porosity characterization, and stress analysis based on FEA improves the interpretation of fracture probability. This provides a more reliable basis for process optimization and design evaluation. These results also serve as the basis for a final discussion on how integrated experimental computational approaches can improve the prediction of failure risk in additive metal production.

4 Conclusions

In this study, an integrated predictive system was developed and evaluated to assess the risk of fatigue failures in Ti-6Al-4V components manufactured by laser powder coating (L-PBF). The experimental results showed that the Ti-6Al-4V specimens achieved yield strengths of 910–940 MPa and ultimate tensile strengths of 1020–1080 MPa, with fatigue lives ranging from 45,000 to 520,000 cycles depending on the applied stress level. XCT characterization revealed porosity levels of 1.8–3.2%, while the predictive model demonstrated good performance with R^2 values of 0.94–0.96 and RMSE values of 0.03–0.05. By combining tensile, fatigue, XCT-based porosity characterization, and finite element analysis (FEA), the study showed that fracture behavior is determined by the combined effects of mechanical properties, internal defects, and localized stress concentrations, rather than by any one parameter.

The predictive model has demonstrated satisfactory effectiveness when comparing experimental and simulation variables with the observed failure-related response, indicating that the integrated approach provides a useful basis for assessing the risk of failure in components manufactured using additional technologies. These results highlight the importance of combining mechanical testing with defect characterization and stress analysis to obtain a more realistic assessment of the structural reliability of L-PBF Ti-6Al-4V parts.

References

[1] L. Zhou *et al.*, "Additive manufacturing: a comprehensive review," *Sensors*, vol. 24, no. 9, p. 2668, 2024.

[2] D. Gu, X. Shi, R. Poprawe, D. L. Bourell, R. Setchi, and J. Zhu, "Material-structure-performance integrated laser-metal additive manufacturing," *Science*, vol. 372, no. 6545, p. eabg1487, 2021.

[3] A. Alfaify, M. Saleh, F. M. Abdullah, and A. M. Al-Ahmari, "Design for additive manufacturing: A systematic review," *Sustainability*, vol. 12, no. 19, p. 7936, 2020.

[4] R. Jemghili, A. Ait Taleb, and M. Khalifa, "A bibliometric indicators analysis of additive manufacturing research trends from 2010 to 2020," *Rapid Prototyping Journal*, vol. 27, no. 7, pp. 1432-1454, 2021.

[5] J. Butt, "Exploring the interrelationship between additive manufacturing and Industry 4.0," *Designs*, vol. 4, no. 2, p. 13, 2020.

[6] J. Jiang, "A novel fabrication strategy for additive manufacturing processes," *Journal of Cleaner Production*, vol. 272, p. 122916, 2020.

[7] J. Savolainen and M. Collan, "How additive manufacturing technology changes business models?–review of literature," *Additive manufacturing*, vol. 32, p. 101070, 2020.

[8] Z. Jin, Z. Zhang, K. Demir, and G. X. Gu, "Machine learning for advanced additive manufacturing," *Matter*, vol. 3, no. 5, pp. 1541-1556, 2020.

[9] N. Asnafi, "Metal additive manufacturing—State of the art 2020," vol. 11, ed: MDPI, 2021, p. 867.

[10] H. D. Vora and S. Sanyal, "A comprehensive review: metrology in additive manufacturing and 3D printing technology," *Progress in additive manufacturing*, vol. 5, no. 4, pp. 319-353, 2020.

[11] Y. Wang, Y. Zhou, L. Lin, J. Corker, and M. Fan, "Overview of 3D additive manufacturing (AM) and corresponding AM composites," *Composites Part A: Applied Science and Manufacturing*, vol. 139, p. 106114, 2020.

[12] A. Aramian, N. Razavi, Z. Sadeghian, and F. Berto, "A review of additive manufacturing of cermets," *Additive Manufacturing*, vol. 33, p. 101130, 2020.

[13] H. Syah, J. Irmansyah, L. Hulfian, and M. R. Lubis, "Hybrid learning space as an alternative for physical education learning post Covid-19 pandemic," *International Journal of Human Movement and Sports Sciences*, vol. 10, no. 5, pp. 1047-1059, 2022.

[14] C. Wang, X. P. Tan, S. B. Tor, and C. Lim, "Machine learning in additive manufacturing: State-of-the-art and perspectives," *Additive Manufacturing*, vol. 36, p. 101538, 2020.

[15] R. Arora, P. K. Arora, H. Kumar, and M. Pant, "Additive manufacturing enabled supply chain in combating COVID-19," *Journal of Industrial Integration and Management*, vol. 5, no. 04, pp. 495-505, 2020.

[16] H. Turkcan, S. Z. Imamoglu, and H. Ince, "To be more innovative and more competitive in dynamic environments: The role of additive manufacturing," *International Journal of Production Economics*, vol. 246, p. 108418, 2022.

[17] M. Alhijazi, Q. Zeeshan, Z. Qin, B. Safaei, and M. Asmael, "Finite element analysis of natural fibers composites: A review," *Nanotechnology Reviews*, vol. 9, no. 1, pp. 853-875, 2020.

[18] S. Shivakumar, V. S. Kudagi, and P. Talwade, "Applications of finite element analysis in dentistry: A review," *Journal of International Oral Health*, vol. 13, no. 5, pp. 415-422, 2021.

[19] S. David Müzel, E. P. Bonhin, N. M. Guimarães, and E. S. Guidi, "Application of the finite element method in the analysis of composite materials: A review," *Polymers*, vol. 12, no. 4, p. 818, 2020.

[20] O. Daqiq, B. van Minnen, F. K. L. Spijkervet, F. W. Wubs, G. Lunter, and C. C. Roossien, "Finite element analysis of mandibular fracture fixation authenticated by 3D printed mandible mechanical testing," *Scientific Reports*, vol. 15, no. 1, p. 14655, 2025.

[21] A. Munjiza *et al.*, "Structural applications of the combined finite–discrete element method," *Computational particle mechanics*, vol. 7, no. 5, pp. 1029-1046, 2020.

[22] X. Geng, L. Ma, C. Liu, C. Zhao, and Z. Yue, "A FEM study on mechanical behavior of cellular lattice materials based on combined elements," *Materials Science and Engineering: A*, vol. 712, pp. 188-198, 2018.

[23] D. Trindade *et al.*, "Material Performance Evaluation for Customized Orthoses: Compression, Flexural, and Tensile Tests Combined with Finite Element Analysis," *Polymers*, vol. 16, no. 18, p. 2553, 2024.

[24] Y. Zhang, H. Xu, R. Peng, Y. Lu, and L. Zhu, "The state of the art of finite element analysis in mechanical clinching," *International Journal of Precision Engineering and Manufacturing-Green Technology*, vol. 9, no. 4, pp. 1191-1214, 2022.

[25] Y. Shokrollahi *et al.*, "Finite element-based machine learning model for predicting the mechanical properties of composite hydrogels," *Applied Sciences*, vol. 12, no. 21, p. 10835, 2022.

[26] F. L. Palombini, E. L. Lautert, J. E. d. A. Mariath, and B. F. de Oliveira, "Combining numerical models and discretizing methods in the analysis of bamboo parenchyma using finite element analysis based on X-ray microtomography," *Wood Science and Technology*, vol. 54, no. 1, pp. 161-186, 2020.

[27] M. Smolnicki, S. Duda, P. Stabla, and T. Osiecki, "Mechanical investigation on interlaminar behaviour of inverse FML using acoustic emission and finite element method," *Composite Structures*, vol. 294, p. 115810, 2022.

[28] S. Baragetti and E. V. Arcieri, "Study of impact phenomena for the design of a mobile anti-terror barrier: Experiments and finite element analyses," *Engineering Failure Analysis*, vol. 113, p. 104564, 2020.

[29] W. Webo, L. M. Masu, and P. K. Nziu, "Finite element analysis and experimental approaches of mono and hybrid nanocellulosic composites under tensile test," *Materials Research Express*, vol. 9, no. 2, p. 020001, 2022.

[30] E. Diz-Mellado *et al.*, "Non-destructive testing and Finite Element Method integrated procedure for heritage diagnosis: The Seville Cathedral case study," *Journal of Building Engineering*, vol. 37, p. 102134, 2021.

[31] H. Javidrad, B. Koc, H. Bayraktar, U. Simsek, and K. Gunaydin, "Fatigue performance of metal additive manufacturing: a comprehensive overview," *Virtual and Physical Prototyping*, vol. 19, no. 1, p. e2302556, 2024.

[32] Ö. Karakaş, F. B. Kardeş, P. Foti, and F. Berto, "An overview of factors affecting high-cycle fatigue of additive manufacturing metals," *Fatigue & Fracture of Engineering Materials & Structures*, vol. 46, no. 5, pp. 1649-1668, 2023.

[33] S. Afazov, A. Serjouei, G. J. Hickman, R. Mahal, D. Goy, and I. Mitchell, "Defect-based fatigue model for additive manufacturing," *Progress in Additive Manufacturing*, vol. 8, no. 5, pp. 1059-1066, 2023.

[34] Z. Zhan and H. Li, "Machine learning based fatigue life prediction with effects of additive manufacturing process parameters for printed SS 316L," *International Journal of Fatigue*, vol. 142, p. 105941, 2021.

[35] A. Fatemi *et al.*, "Fatigue behaviour of additive manufactured materials: An overview of some recent experimental studies on Ti-6Al-4V considering various processing and loading direction effects," *Fatigue & fracture of engineering materials & structures*, vol. 42, no. 5, pp. 991-1009, 2019.

[36] R. VanSickle, D. Foehring, H. B. Chew, and J. Lambros, "Microstructure effects on fatigue crack growth in additively manufactured Ti–6Al–4V," *Materials Science and Engineering: A*, vol. 795, p. 139993, 2020.

[37] N. Macallister, T. Becker, and D. Blaine, "Fracture mechanics-based fatigue life assessment of additively manufactured Ti-6Al-4V," Stellenbosch: Stellenbosch University, 2024.

[38] B. Naab, S. Ramachandran, W. Mirihanage, and M. Celikin, "Fatigue prediction through quantification of critical defects and crack growth behaviour in additively manufactured Ti-6Al-4V alloy," *Materials Science and Engineering: A*, vol. 903, p. 146658, 2024.

[39] J. Chen and Y. Liu, "Fatigue property prediction of additively manufactured Ti-6Al-4V using probabilistic physics-guided learning," *Additive Manufacturing*, vol. 39, p. 101876, 2021.

[40] J. Horňas *et al.*, "Modelling fatigue life prediction of additively manufactured Ti-6Al-4V samples using machine learning approach," *International Journal of Fatigue*, vol. 169, p. 107483, 2023.

[41] C. Ni *et al.*, "Recent advance in laser powder bed fusion of Ti–6Al–4V alloys: microstructure, mechanical properties and machinability," *Virtual and Physical Prototyping*, vol. 20, no. 1, p. e2446952, 2025.

[42] E. Maleki, S. Bagherifard, and M. Guagliano, "Application of artificial intelligence to optimize the process parameters effects on tensile properties of Ti-6Al-4V fabricated by laser powder-bed fusion," *International Journal of Mechanics and Materials in Design*, vol. 18, no. 1, pp. 199-222, 2022.

[43] K. Huang, C. Kain, N. Diaz-Vallejo, Y. Sohn, and L. Zhou, "High throughput mechanical testing platform and application in metal additive manufacturing and process optimization," *Journal of Manufacturing Processes*, vol. 66, pp. 494-505, 2021.